Mol Biotechnol (2013) 55:277–287
DOI 10.1007/s12033-013-9679-z

RESEARCH

Molecular Cloning, Expression, and In Silico Structural Analysis of Guinea Pig IL-17

Vijaya R. Dirisala · Amminikutty Jeevan · Suresh K. Ramasamy · David N. McMurray

Published online: 29 June 2013

Abstract Interleukin-17A (IL-17A) is a potent proinflammatory cytokine and the signature cytokine of Th17 cells, a subset which is involved in cytokine and chemokine production, neutrophil recruitment, promotion of T cell priming, and antibody production. IL-17 may play an important role in tuberculosis and other infectious diseases. In preparation for investigating its role in the highly relevant guinea pig model of pulmonary tuberculosis, we cloned guinea pig IL-17A for the first time. The complete coding sequence of the guinea pig IL-17A gene (477 nucleotides; 159 amino acids) was subcloned into a prokaryotic expression vector (pET-30a) resulting in the expression of a 17 kDa recombinant guinea pig IL-17A protein which was confirmed by mass spectrometry analysis. Homology modeling of guinea pig IL-17A revealed that the three-dimensional structure resembles that of human IL-17A. The secondary structure predicted for this protein showed the presence of one extra helix in the N-terminal region. The expression profile of IL-17A was analyzed quantitatively in spleen, lymph node, and lung cells from BCG-vaccinated guinea pigs by real-time PCR. The guinea pig IL-17A cDNA and its recombinant protein will serve as valuable tools for molecular and immunological studies in the guinea pig model of pulmonary TB and other human diseases.

Keywords Th-17 · IL-17A · Guinea pig · Protein

Introduction

Tuberculosis (TB) remains a major life threatening disease with approximately one-third of world population latently infected with *Mycobacterium tuberculosis* (*M. tb*) [1]. The only available vaccine Bacillus Calmette–Guérin (BCG) does not afford complete protection and shows variable efficacy (0–80 %) [2]. New TB vaccines are in various phases of pre-clinical development and several are currently in clinical trials [3]. Novel TB vaccines need to be tested in animal models that mimic human TB. The guinea pig has been used extensively as a gold standard for testing novel vaccine candidates during pre-clinical development because it mimics human TB in the formation of granulomatous lesions which undergo necrosis, extrapulmonary dissemination, and vaccine induced protection [4–6]. The major limitation of the guinea pig model is the shortage of readily available immunological reagents that has hampered its use in TB and many other important diseases [7]. In order to develop molecular and immunological reagents, our laboratory has cloned and expressed guinea pig cytokine and chemokine genes such as interleukin-8 [8], regulated upon activation, normal T-cell expressed, and secreted [9], tumor necrosis factor-alpha (TNF-α) [10], interferon-gamma (IFN-γ) [11], interleukin-4 [12],

Electronic supplementary material The online version of this article (doi:10.1007/s12033-013-9679-z) contains supplementary material, which is available to authorized users.

V. R. Dirisala · A. Jeevan · D. N. McMurray
Department of Microbial and Molecular Pathogenesis, College of Medicine, Texas A&M Health Science Center, College Station, TX 77843-1114, USA

Present Address:
V. R. Dirisala (✉)
Division of Hematology, Department of Internal Medicine, Ohio State University Medical Center, Columbus, OH 43210, USA
e-mail: drdirisala@gmail.com

S. K. Ramasamy
Division of Chemistry and Chemical Engineering, California Institute of Technology (Caltech), Pasadena, CA 91125, USA

interleukin-10 [13], interleukin-1beta and monocyte chemo attractant protein-1 [14].

The interplay of various T cell-mediated immune responses is crucial in combating *M. tb* infection. Although it has been well established that Th1 cells and cytokines such as IFN-γ and TNF-α play an important role in cell-mediated immune responses to *M. tb* [15], other T cell subsets and cytokines are clearly involved. Th17 cells have been implicated in both the resistance to, and pathology of, *M. tb* infection [16]. Interestingly, early *M. tb*-induced IL-17 production appears to orchestrate granuloma formation and control of bacterial growth [17], while higher levels of IL-17 promote inflammation, neutrophil recruitment and tissue damage. During the chronic phase of TB, the equilibrium between Th1 and Th17 responses may be essential to control bacterial growth and constrain immunopathology [18]. For example, TNF-α, IL-12(p40), and IL-17A production upon ex vivo stimulation of cells with an immunodominant mycobacterial antigen, TB10.4, allowed investigators to discriminate between active TB disease and latent infection in a West African cohort [19].

IL-17A is an important proinflammatory cytokine and the signature cytokine of Th17 cells, a subset which is involved in cytokine and chemokine production, neutrophil recruitment, promotion of T-cell priming and antibody production [20–22]. IL-17A gene knockout mice failed to develop mature granulomas in the *Mycobacterim bovis* BCG-infected lung [17]. Cloning and expression of the guinea pig IL-17A would allow a deeper understanding of the contributions of Th17 cells to the response to vaccination and infection. Here, we report for the first time the molecular cloning and expression of recombinant guinea pig (rgp) IL-17.

Materials and Methods

Experimental Animals and Immune Cell Preparations

Specific pathogen-free, random-bred Hartley strain guinea pigs were obtained from a commercial vendor (Charles River Breeding Laboratories, Inc., Wilmington, MA, USA). The animals were housed individually in polycarbonate cages in a temperature and humidity controlled environment with an alternating 12 h light and dark cycle. All procedures were approved by the Texas A&M University Laboratory Animal Care Committee.

Guinea pigs were vaccinated intradermally with 1×10^3 colony forming units (CFU) of *M. bovis* BCG (Danish 1331 Strain, Statens Seruminstitut, Copenhagen, Denmark) on both flanks. Eight to twelve weeks later, they were euthanized and their draining lymph nodes, spleen, and lung digest cells were isolated following our published procedures [23]. Cell viability was determined by the trypan blue exclusion method [24]. Cells (1×10^6 cells per well) were cultured in 24-well plates with either tuberculin (Purified Protein Derivative, PPD at 25 μg/mL; a gift from Dr. Saburo Yamamoto, BCG Laboratories, Tokyo, Japan), live BCG (MOI 1:5), or medium alone for 24 h. The cells were lysed with RLT buffer (Qiagen, Valencia, CA) and stored at −80 °C for further processing. RNA was extracted using the RNeasy mini kit (Qiagen, Valencia, CA). The quality of RNA was analyzed by bioanalyzer (Agilent Technologies, Palo Alto, CA), and the quantity was measured using Nanodrop (Nanodrop Technologies, Wilmington, DE) [25].

Cloning of Guinea Pig IL-17

The human IL-17A cDNA sequence (NM_002190) from Genbank was subjected to in silico analysis by Basic Linear Alignment Search Tool (BLAST) against the available guinea pig genome sequence in Genbank. The in silico comparison generated a guinea pig IL-17A cDNA sequence which was subjected to confirmation by amplifying the reverse transcribed cDNA that was derived from spleen cells stimulated with PPD and amplified using primer pairs (forward: 5′-GCT GCT GAG TCT GAT GGC TA-3′; and reverse: 5′-CCA CGG TCA CCT TCA TCT TC-3′). PCR amplification was performed using Phusion high fidelity DNA polymerase (NEB, Beverly, MA). The PCR amplification conditions were 33 cycles of 98 °C for 10 s, annealing temperature of 55 °C for 20 s, extension of 1 min at 72 °C with an initial denaturation of 98 °C for 30 s, plus a final extension of 72 °C for 4 min. Using the partially deduced guinea pig IL-17A sequence information, it was decided to use the same template and apply rapid amplification of cDNA ends (RACE) methodology (Gene Racer kit; Invitrogen, Carlsbad, CA) to obtain the complete 5′ and 3′ ends of the IL-17A sequence.

Five microgram of total RNA isolated from spleen cells stimulated with PPD was chosen as starting material and was treated with calf intestinal phosphatase to remove the 5′ phosphates. The dephosphorylated RNA was treated with tobacco acid pyrophosphatase which leaves a 5′ phosphate required for ligation to the GeneRacer RNA oligo (5′-GCT GTC AAC GAT ACG CTA CGT AAC GGC ATG ACA GTG (T)24-3′). The GeneRacer RNA oligo was ligated to the 5′ phosphate using T4 RNA ligase which was then reverse transcribed using Superscript III enzyme (Invitrogen) to obtain the first strand cDNA.

The first strand cDNA was amplified using a gene specific primer (forward: 5′-GCT GCT GAG TCT GAT GGC TA-3′) and the Gene Racer 3′ primer (reverse: 5′-GCT GTC AAC GAT ACG CTA CGT AAC G-3′). The amplification conditions were 33 cycles of 98 °C for

10 s, annealing temperature of 58 °C for 10 s, extension of 15 s at 72 °C with an initial denaturation of 98 °C for 30 s, plus a final extension of 72 °C for 7 min. The 3′ RACE product was run on a 1.5 % agarose gel and eluted using the Qiaquick gel extraction kit (Qiagen). The eluted PCR product was subjected to nested PCR using the 5′ gene specific primer (TGA TGG CTA CAG TGA AGG CA) and the Gene Racer 3′ nested primer (5′-CGC TAC GTA ACG GCA TGA CAG TG-3′). The amplification conditions utilizing a touchdown PCR were an initial denaturation of 94 °C for 2 min, followed by 5 cycles of 94 °C for 30 s, 69 °C for 1 min, 5 cycles of 94 for 30 s, 66 °C for 1 min, and 25 cycles of 94 °C for 30 s, 60 °C for 30 s plus a final extension of 68 °C for 10 min. The 3′ RACE product was subjected to DNA sequencing using fluorescent-labeled dideoxy nucleotide terminators with Big Dye version 3.1 and ABI 3130 xI automated sequencers (Applied Biosystems, Foster City, CA).

To obtain 5′ ends, the first strand cDNA was amplified using a forward Gene Racer primer (5′-CGA CTG GAG CAC GAG GAC ACT GA-3′) and reverse gene specific primer (5′-CCA CGG TCA CCT TCA TCT TC-3′). The 5′ RACE product obtained was run on a 1.5 % agarose gel, eluted and subjected to nested PCR using the forward Gene Racer nested primer (5′-GGA CAC TGA CAT GGA CTG AAG GAG TA-3′) and reverse gene specific primer (5′-GTC ACC TTC ATC TTC TCC AG-3′). The 5′ blunt ended RACE product was ligated into the pCR-Blunt II-TOPO vector (Invitogen) and transformed with One Shot Top10 chemically competent *E. coli* (Invitrogen). Plasmid DNA was isolated from the transformants and subjected to restriction analysis and confirmation by DNA sequencing using the M13 forward (−20) priming site present in the vector. The chromatogram sequences obtained for both the 5′ and 3′ RACE products were inspected visually and aligned by CLUSTALW (http://www.ebi.ac.uk/Tools/msa/clustalw2/) to obtain the complete IL-17A nucleotide sequence. Based on the information deduced from 5′ and 3′ RACE products, the RNA isolated from spleen cells stimulated with PPD was used as a template in obtaining complete coding sequence of guinea pig IL-17 which was confirmed by DNA sequencing from 5′ and 3′ ends prior to cloning into prokaryotic expression vector. The amino acid homology of gp IL-17A sequences with that from other species was determined by CLUSTALW. Phylogenetic analysis was performed via the maximum likelihood method using MEGA5 program [26].

Sub-cloning of Guinea Pig IL-17A Gene

The signal peptide region of the guinea pig IL-17A gene was predicted using a bioinformatic tool SignalP [26] and the mature peptide region of the IL-17A gene was amplified by PCR with primer sequences (Invitrogen) containing *Bam*HI and *Hin*dIII recognition sites to facilitate cloning. The forward and reverse primer sequences used for amplification of the IL-17A gene were 5′-TA***G GAT CC***G GAA TAC CAA TCC CAC GAA AT CCA -3′ and 5′-TA***A AGC TT***C TGG CCA TTG TTA TTT CCC A-3′. The underlined parts of primer sequences represent the nucleotide sequence of the gene whereas 5′ overhangs (bolded and italicized) are restriction sites designed to enable cloning.

PCR amplification conditions of the IL-17A gene were 33 cycles of 98 °C for 10 s, annealing at 56 °C for 20 s, extension for 1 min at 72 °C with an initial denaturation of 98 °C for 30 s, plus a final extension at 72 °C for 4 min. The PCR product that was obtained for the IL-17A gene was digested with *Bam*HI and *Hin*dIII restriction enzymes (NEB) and ligated into the pET-30a(+) vector containing the same restriction sites (Novagen, Madison, WI). The ligation mixtures were transformed with chemically competent Top 10 F *E. coli* (Novagen). Five transformants were randomly selected for plasmid DNA isolation and analyzed for the presence of inserts by restriction analysis. Bidirectional sequencing of the transformants was performed. Plasmid DNA from two of the confirmed transformants was transformed into chemically competent Rosetta 2(De3) *E. coli* cells (Novagen).

Expression of rgp IL-17A

The colonies were inoculated into 3 milliliters (mL) of LB broth containing kanamycin (15 μg/mL) and chloramphenicol (34 μg/mL) and grown overnight at 37 °C on a shaking incubator. That culture was added to 50 ml of identical culture medium and then incubated with shaking at 37 °C. When the OD_{600} of the cultures reached 0.7, protein expression was induced by adding Isopropyl-β-D-thiogalactoside (IPTG) (Sigma, St. Louis, MO) to a final concentration of 1.0 mM. After induction with IPTG, the incubation continued for 5 h at 37 °C. The cells were harvested by centrifugation and the pellet was resuspended in 5 mL lysis buffer (50 mM NaH_2PO_4, 300 mM NaCl and 10 mM Imidazole, pH 8.0) followed by addition of lysozyme (Sigma) at 1 mg/mL and incubation on ice for 30 min. The sample was subjected to sonication (Misonix Inc., Farmingdale, NY) and was centrifuged to obtain the cleared lysate and the pellet. The induced/expressed proteins in the cleared lysate and pellet fractions were analyzed by sodium dodecyl sulfate (SDS)-polyacrylamide gel electrophoresis (PAGE) using a pre-cast Novex 10–20 % Tricine gel (Invitrogen) to determine the solubility of the target protein.

Rgp IL-17A Protein Purification

The pellet was lysed under denaturing conditions following the Qiaexpressionist protocol in the presence of 10 mM benzamidine (Sigma) to obtain the cleared lysate which was then centrifuged at 10,000 relative centrifugal force for 30 min. The supernatant collected after centrifugation was mixed with 50 % nickel–nitrilotriacetic acid slurry (Ni–NTA) (Qiagen) in a ratio of 1 ml: 4 ml, set on rotary shaker for 1 h at room temperature. The immobilized protein was washed and eluted in elution buffer (100 mM NaH_2PO_4, 10 mM Tris–Cl, pH 4.5) using polypropylene columns (Qiagen) in the presence of 8 M urea. Renaturation of the denatured protein was carried out by gentle drop-wise addition of 10 ml of eluted protein to 100 ml of dilution buffer (50 mM Tris, 50 mM NaCl, pH 8.0) containing 14 µl of ß-mercaptoethanol in the absence of urea. The folded protein solution was left for 3 h at room temperature and placed at 4 °C overnight. Protein was concentrated in Amicon Ultra-15 centrifugal filter devices with a 3 kDa cutoff (Millipore, Bedford, MA) and the concentrated protein content was determined by the Bradford assay (Bio-Rad, Hercules, CA).

Mass Spectrometry Analysis of rgp IL-17A

The eluted and concentrated IL-17A protein (approximately 50 µg) was digested with 2 U of enterokinase enzyme (Novagen) and incubated at room temperature for 4 h or 14 h. The digested IL-17A protein was run on a Novex 10–20 % tricine gel (Invitrogen). The protein of interest that appeared as a band on the gel was excised and digested with mass spectrometry grade trypsin [27]. Prior to digestion with trypsin, in silico digestion analysis was performed for the IL-17A protein sequence to determine the pattern of peptides. In-gel mass spectra were recorded by matrix-assisted laser desorption ionization time of flight (MALDI-TOF) (Shimadzu/Kratos) with delayed extraction and reflection capabilities for high mass accuracy analysis of peptides at the Protein Chemistry Laboratory of Texas A&M University.

Homology Modeling of Guinea Pig IL-17A

To predict the three-dimensional structure of guinea pig IL-17A protein, a sequence similarity search was carried out by BLAST analysis to find homologous protein sequences, structures of which have been deposited in the Protein Data Bank (PDB). The atomic coordinates of the structure of human IL-17A in complex with a potent, fully human neutralizing antibody (pdbcode: 2vxs) was obtained from the PDB. The chain A of this X-ray structure was used to build the three-dimensional models of the protein. Modeller-Modweb (https://modbase.compbio.ucsf.edu/scgi/modweb.cgi) and Swiss-Prot model (http://swissmodel.expasy.org) were used in building the three-dimensional structure of the guinea pig IL-17A protein. The homology model coordinates were then energy minimized with the Schrodinger Macromodel module (Macromodel, version 9.8, Schrodinger, LLC, New York, NY) using OPLS_2001 force field until the structures reached the final derivative of 0.001 kcal/mol. The stereochemical qualities of the models were checked using the program PROCHECK [28] and Ramachandran Plots [29] were drawn. The visualization of the above studies was done using Pymol (http://www.pymol.org; DeLano Scientific LLC, USA). The conserved residues of IL-17A structure were analyzed by ConSurf server (http://consurf.tau.ac.il/).

Real-Time PCR Analysis for IL-17A mRNA

Total RNA isolated from the stimulated and unstimulated guinea pig spleen, lymph node, and lung digest cells using the RNeasy mini columns (Qiagen) was subjected to reverse transcription using TaqMan Reverse Transcription reagents. Real-time-PCR (RT-PCR) was performed using SYBR Green I dye (Applied Biosystems, Foster City, CA) and analyzed using the ABI Prism 7700 sequence detector. RT-PCR primers for guinea pig IL-17A and HPRT were designed with Primer Express software (Applied Biosystems). The forward and reverse primer sequences for IL-17A were 5′-CGT CCC ATC CAG CAA GA-3′ and 5′-AGC GGG CAG TTC TGA GGT T-3′ based upon the nucleotide sequence presented in this manuscript. The forward and reverse primer sequences for the following guinea pig genes were the same as those used in our previous studies [11, 12]: housekeeping gene HPRT (5′-AGG TGT TTA TCC CTC ATG GAC TAA TT-3′; 5′-CCT CCC ATC TCC TTC ATC ACA T), IFN-γ (5′-ATT TCG GTC AAT GAC GAG CAT-3′; 5′-GTT TCC TCT GGT TCG GTG ACA-3′) and IL-4 (5′-GCA ACC ACC ACA CCT TGC AAG AAA-3′; 5′-AGA AGT CTT TCA GTG TCG TCT GCC-3′). Fold induction of mRNA was calculated from the threshold cycle values (Ct) normalized to HPRT and then to unstimulated cultures of the same cell type.

Statistical Analysis

The real-time RT-PCR results are expressed as the mean ± SEM (Standard error of the mean) of 5-10

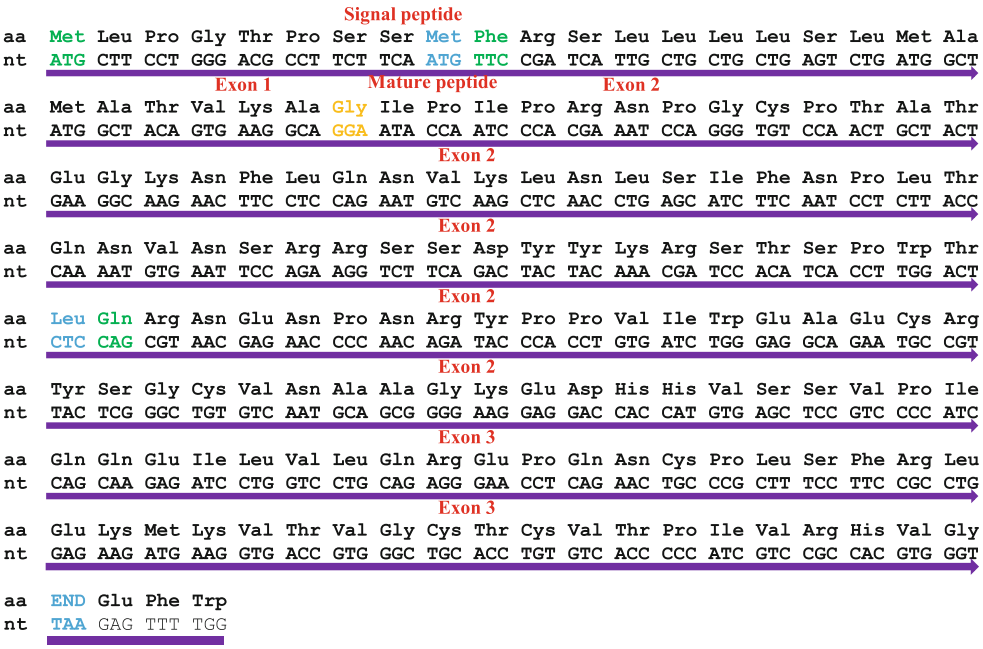

Fig. 1 Nucleotide (nt) and deduced amino acid (aa) sequence for guinea pig Interleukin-17A (IL-17A). The guinea pig IL-17A gene contains 3 exons. The start and end of the amino acids in each of the exons are marked in *green* and *blue*, respectively. ATG (methionine) denotes the initiation codon and TAA denotes the stop codon for the gene. Mature peptide region of the protein starts at 24th aminoacid glycine marked in *yellow* and prior to that is the signal peptide region (Color figure online)

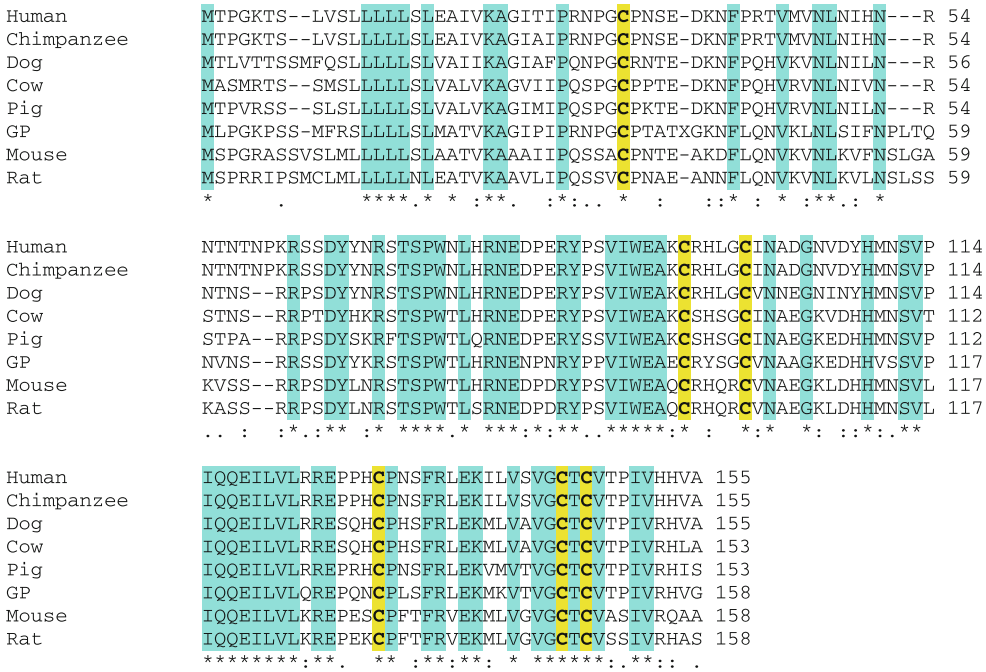

Fig. 2 Amino acid sequence comparison of IL-17A from different species. Amino acid sequences of human (NP_002181), chimpanzee (XP_527408), cow (NP001008412), mouse (NP_034682), rat (NP_001100367), pig (NP_001005729), dog (NP_001159350), and guinea pig (JN020146). Amino acid substitutions found to be conservative or semi-conservative by ClustalW are denoted as (*colon*) and (*dot*), respectively. *Shading* shows identical amino acids and the *numbers on the right* represent the position of the amino acids. The stop codon is not shown in the figure for any of the amino acid sequences which makes them shorter by an amino acid. *Yellow shading* emphasizes conserved cysteine residues (Color figure online)

animals. The data were analyzed by the GraphPad Prism (version 4.03, 2005; GraphPad, Inc., San Diego, CA) software package for the Mann–Whitney non-parametric test to compare results between PPD and BCG-stimulated cultures. P values of <0.05 were considered statistically significant.

Table 1 The percentage of amino acid similarity of the IL-17 gene from multiple species

Species	Chimpanzee	Cow	Mouse	Rat	Pig	Dog	Guinea pig
Human	99	74	63	58	73	76	65
Chimpanzee		74	63	58	73	77	65
Cow			66	64	83	77	66
Mouse				86	64	63	61
Rat					64	63	60
Pig						72	66
Dog							67

Genbank accession numbers of IL-17 amino acid sequences from mammalian species: human (NP_002181), chimpanzee (XP_527408), cow (NP00 1008412), mouse (NP_034682), rat (NP_001100367), pig (NP_001005729), dog (NP_001159350), and guinea pig (JN020146)

Results

Cloning of Guinea Pig IL-17A cDNA and Sequence Analysis

Identification of the complete nucleotide sequence of the gpIL-17A gene from the widely used random-bred Hartley strain of guinea pigs was facilitated by the availability of genomic sequences from inbred Strain 2 guinea pigs in the NCBI database accompanied by 5′ and 3′ RACE methodology. Successful amplification of the IL-17A gene from the reverse transcribed cDNA of PPD-stimulated guinea pig spleen cells generated a PCR product of approximately 400 bp that was the same as that deduced by in silico analysis and was confirmed to be the partial coding sequence of guinea pig IL-17A. The complete nucleotide sequence of guinea pig IL-17A was determined by RACE methodology using a higher concentration of the same template. The concentrations of both the 5′ and 3′ RACE products obtained prior to nested PCR amplification were too low to allow either sequencing or cloning into the TOPO vector. Therefore, nested PCR was performed for both the 5′ and 3′ RACE products. All of the six randomly selected transformants containing the 5′ RACE PCR product obtained after nested PCR and cloned in the Pcr-Blunt II-Topo vector contained the gene of interest for a recombination percentage of 100 %. The 5′ and 3′ RACE products obtained by DNA sequencing for the gpIL-17A gene when aligned by CLUSTALW generated a nucleotide sequence of 887 bp in length. The complete open reading frame of guinea pig IL-17A cDNA consists of 477 nucleotides which encodes a protein of 159 amino acid residues (Fig. 1). The translated guinea pig IL-17A sequence has 3 amino acid insertions at different sites in comparison with that of humans and chimpanzees which makes it 9 nucleotides longer. The deduced amino acid sequence of our guinea pig IL-17A cDNA showed higher homology with the IL-17A cDNA from dog and cow in comparison with other species (Fig. 2; Table 1). The percentage of amino acid similarity between guinea pig IL-17A and that of other species ranges from 60 to 67 %. As expected, amino acid sequences of IL-17A from humans and chimpanzees were 99 % homologous whereas the IL-17A gene sequence from closely related species mouse and rat were 86 % homologous but were grouped together in the phylogenic tree (Fig. 3). The guinea pig IL-17A cDNA sequence was submitted to Genbank with the accession number JQ315117.

Confirmation and Expression of IL-17A

All of the five putative transformants randomly selected for the IL-17A gene cloned in the pET-30a(+) vector contained the gene of interest when analyzed by restriction analysis or PCR for a recombinant percentage of 100 %. Induction with IPTG resulted in the generation of a protein that was visible as a 17 kDa band corresponding to rgp IL-17A (Fig. 4). Target protein solubility for rgp IL-17A protein showed that it was obtained in the insoluble form and was efficiently purified under denaturing conditions. All the eluted fractions run on SDS-PAGE were of the same size indicating that the eluted fractions contained the protein of interest (Fig. 4).

Confirmation of the Protein by Mass Spectrometry Analysis

Digestion of the purified recombinant IL-17A protein with enterokinase resulted in successful cleavage of the tags, making it possible to obtain the mature peptide region of the protein. There were at least 6 peptides in the spectrum obtained by MALDI-TOF that matched the predicted peptides from the in silico digest analysis of the IL-17 protein. Interestingly, many of the matching peptides were matched only by allowing for modifications (methionine oxidation and carboxymethylation of Cys) which were done intentionally as part of the digestion process. That sequence corresponded to the IL-17A amino acid sequence that we are reporting in this study.

In Silico Structural Confirmation of Guinea Pig IL-17A

The results obtained from homology modeling of guinea pig IL-17A protein showed that the structure of guinea pig IL-17A resembles that of human IL-17A (Figs. S1, S2). Guinea pig IL-17A is structurally similar to cystine knot family of proteins, where three disulfide knots with antiparallel β-strands substructure provide considerable structural stability. The difference between the classical cysteine knot family members and the IL-17A structure is that,

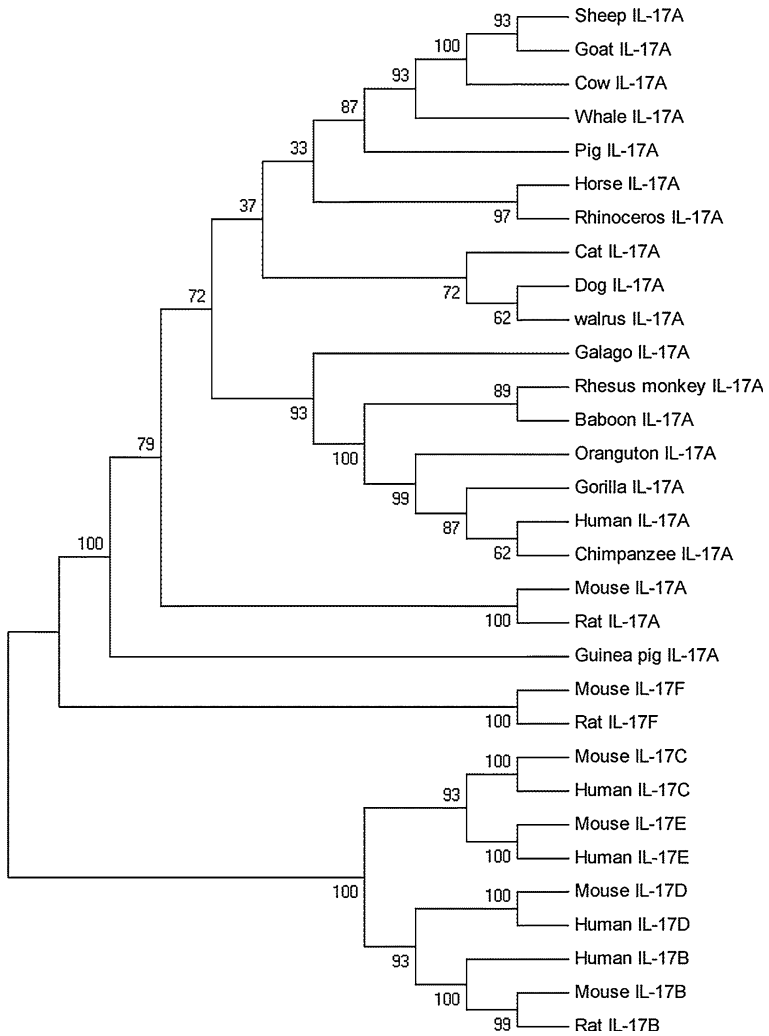

Fig. 3 Phylogenetic analysis of the IL-17A gene based on the nucleotide alignment of the coding sequences from different species. The *numbers* at the *branch nodes* denote the boot strap value after 1,500 replications. Genbank accession numbers of IL-17A nucleotide sequences are human (NM_002190), chimpanzee (XM_527408), cow (NM_001008412), mouse (U43088), rat (NM_001106897), pig (NP_001005729), dog (BAH89243), sheep (XM_004018887), goat (GU269912), killer whale (XM_004285605), white rhinoceros (XM_004424029), horse (NM_001143792), galago (XM_003789640), rhesus monkey (XM_001106391), baboon (XM_003897728), orangutan (XM_002816996), gorilla (XM_004044183), walrus (XM_004415641), rainbow trout (NM_001124169), cat (XM_003986268), and guinea pig (JN020146). Genbank accession numbers of IL-17B nucleotide sequences are human IL-17B (BC113946), mouse IL-17B (BC002271), and rat IL-17B (NM053789). Genbank accession numbers of IL-17C nucleotide sequences are human IL-17C (NM_013278) and mouse IL-17C (NM145834). Genbank accession numbers of IL-17D nucleotide sequences are human IL-17D (BC036243) and mouse IL-17D (AF458063). Genbank accession numbers of IL-17E nucleotide sequences are human IL-17E (AY359127), mouse IL-17E (NM_080729). Genbank accession numbers of IL-17F nucleotide sequences are rat IL-17F (NM_001015011), mouse IL-17F (NM_145856) and human IL-17F (NM_052872)

in the later one the third disulfide bond is absent. Two conserved serine residues have replaced this last pair of cysteine residues. The disulfide bond between the residue Cys97 and Cys147 and also between Cys 102 and Cys 149 were conserved in all species which implies a crucial functional role [30]. The guinea pig IL-17A model structure has the same cystine-knot architecture identified in the crystal structure of human IL-17A (Fig. S4). The secondary structure predicted for this protein (Figs. 5a, S3) indicates the presence of one extra helix in the N-terminal region of the guinea pig protein. With that exception, all other secondary structure elements in the human protein remain intact in guinea pig IL-17A. The crystal structure of human IL17A was reported to be a dimer [30]. As the lower part of the dimer is disordered, the chain is not traceable in the X-ray structure from residue number 99 to 108. So in this region, the predicted models are very different between the modeler and Swiss-Prot model (Fig. S2). Part of the N-terminal region of the protein comprising of 34 residues could not be modeled because of low sequence identify at

that region compared to existing structures from homologous protein sequences in PDB. The superimposed structure between human IL-17A and guinea pig IL-17A models are shown in Fig. S3: and the root-mean-square deviation of 0.44 90 Cα positions. The electrostatic surface calculation suggested that the N-terminal region of the guinea pig IL-17A protein is predominantly represented with positive charges and in the C-terminal region there are a few patches with negative charges (Fig. S5). The Consurf results indicate the presence of many conserved and crucial surface residues in the protein (Fig. 5b). A potential glycosylation site at the 50th amino acid asparagine in the guinea pig IL-17A protein was predicted by web-based tool (http://www.cbs.dtu.dk/services/NetNGlyc/).

IL-17A mRNA Expression Analysis

After BCG vaccination, IFN-γ mRNA levels in the lymph node and spleen cells stimulated with both PPD and live BCG were significantly higher than IL-17A levels ($P < 0.01$). Interestingly, stimulation with live BCG tended to induce higher levels of IL-17A mRNA in the lymph node and lung digest cells compared to PPD, although the differences were not statistically significant ($P > 0.05$). The expression of IFN-γ mRNA was significantly increased after stimulation with PPD compared to live BCG in lymph node and spleen cells. These results suggest that the upregulation of IL-17A and IFN-γ in the cells from BCG-vaccinated guinea pigs is dependent on the type of antigen used for restimulation. It is known that BCG vaccination of guinea pigs increases the ex vivo expression of IFN-γ mRNA but decreases the expression of IL-4 mRNA [11]. There was low expression of IL-4 mRNA expression in these cells which is consistent with the findings published in our previous report (data not shown) [11].

Discussion

The first objective of this study was to decipher the complete nucleotide sequence of the guinea pig IL-17A gene and establish an efficient methodology for rgp IL-17A protein expression. The guinea pig IL-17A gene sequence when analyzed by NCBI Spidey showed that it contains 3 exons separated by introns of approximately 1.2 Kb in length. Of the three exons, exon 3 is the longest with 238 nucleotides and exon 1 is the shortest with 27 nucleotides (Fig. 1). Comparative analysis of IL-17A amino acid sequences chosen for multiple alignment showed that the amino acid sequences of IL-17A from guinea pig, mouse, and rat are of equal length containing 158 amino acids and are longer in length compared to that from other species (Fig. 2). The guinea pig IL-17A gene shows 65 % homology at the amino acid level with human IL-17A (Table 1) but it is only 36 % homologous to human IL-17F (Genbank accession number NM_052872). The homology of mouse IL-17A with that of mouse IL-17F is 50 % [22]. Interestingly IL-17B, IL-17 C, IL-17D, and IL-17E from human and mouse were grouped together during the phylogenetic analysis (Fig. 3). The guinea pig IL-17A model structure has the same Cystine-knot architecture identified in the crystal structure of human IL-17A (Fig. S4). Obtaining recombinant proteins in the insoluble form was once regarded as a bottleneck in protein expression strategies but recent studies suggest that obtaining proteins as insoluble aggregates in inclusion bodies tends to yield a protein of higher purity [31]. Like the rgp IFN-γ and IL-10 proteins that were obtained in the insoluble form and efficiently denatured and renatured to retain biological activity [11, 13, 32], rgp IL-17A was also efficiently denatured and renatured. The mRNA expression as well as other T cell responses in the lung digest cells differ from that of spleen or lymph node.

The activity of rgp IL-17A will be measured by its ability to induce interleukin 6 (IL-6), IL-1β and TNF-α production in guinea pig keratinocytes and fibroblasts as has been demonstrated in humans or mice [33]. Since this is the first identified and cloned member of the guinea pig Th-17 family, cloning of other Th-17 members will enable us to have a deeper understanding of the individual functions and interactions among the members. The ability of rgp IL-17A to stimulate the production of proinflammatory IL-1β and TNF-α by guinea pig macrophages will be assessed as reported for human macrophages [34]. Also the ability of these cytokines to synergize with IL-17A to augment the synthesis of neutrophil-specific chemokines and granulocyte–macrophage colony-stimulating factor [35–37] will be evaluated.

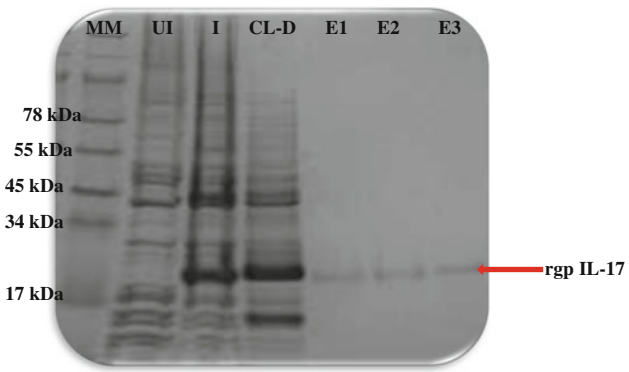

Fig. 4 SDS-PAGE analysis of recombinant IL-17A from one of the clone after IPTG induction at 5 h interval and the cleared lysates obtained under denaturing conditions. The purified fractions of the protein are also shown in the figure. *MM* molecular weight marker, *UI* uninduced samples, *I* induced samples, *D-CL* cleared lysate under denaturing conditions and *E* eluted fractions

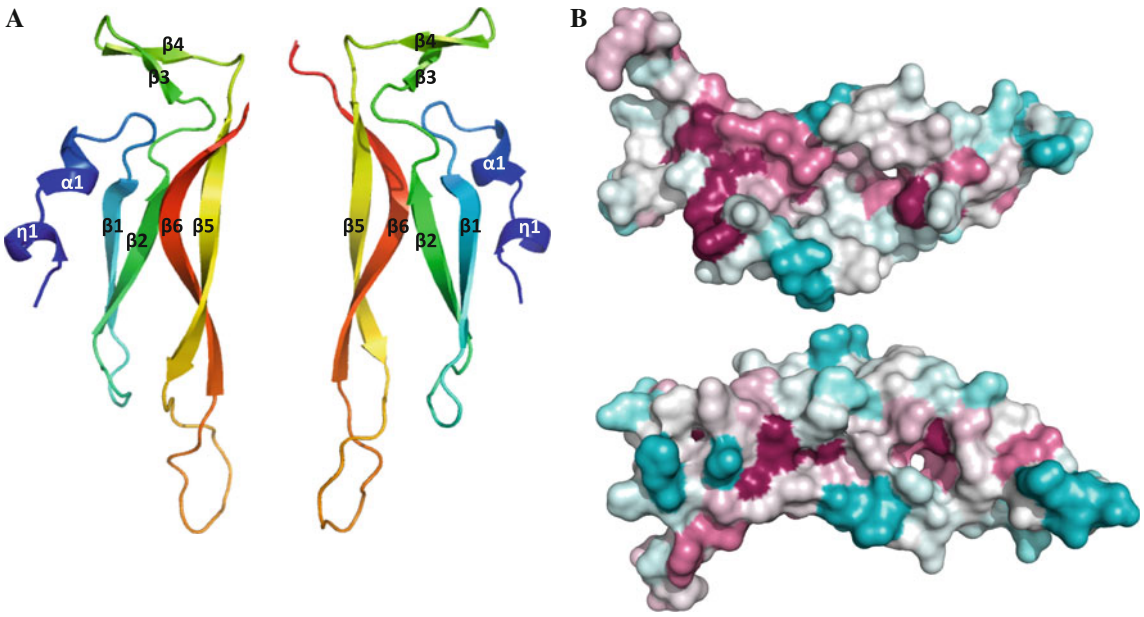

Fig. 5 **a** Cartoon diagram of IL-17A from *Cavia porcellus* viewed from front and back which is color-ramped from N to C terminus (*blue* to *red*). **b** The front and back view of conserved residue on the surface of guinea pig IL-17A. Surfaces are *colored* based on surface conservation calculated by the ConSurf server (http://consurf.tau.ac.il/) as a heat map with *red* being the most conserved and *blue* being the least conserved (Color figure online)

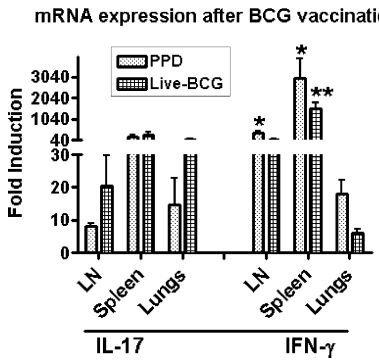

Fig. 6 IFN-γ and IL-17A mRNA expression in the stimulated cells of *M. bovis* BCG-vaccinated guinea pigs. Guinea pigs were vaccinated intradermally with 1×10^3 CFU of *M. bovis* BCG on both flanks. Eight to twelve weeks later, they were euthanized and their draining lymph nodes, spleen, and lung digest cells were stimulated with PPD (25 μg/ml) or live BCG (MOI: 0.5) for 24 h. The RNA was subjected to real-time RT-PCR and the fold induction of mRNA expression was calculated from the threshold cycle (Ct) values normalized to HPRT Ct values and to the unstimulated cells. The results are mean ± standard error of mean from five guinea pigs. The differences in the fold induction between PPD- and BCG-stimulated groups were assessed by the Kruskal–Wallis test followed by Dunn's post hoc test ($*P < 0.05$)

We have shown earlier that lung macrophages and peritoneal macrophages from BCG-vaccinated guinea pigs differed with respect to their cytokine responses to ex vivo stimulation [38, 39] representing a protective immunoregulatory mechanism within the lung. Restimulation ex vivo of all three cell types with both PPD and BCG resulted in marked upregulation of both IL-17A and IFNγ mRNA (Fig. 6). It is interesting to note that lymph node and spleen cells from BCG-vaccinated guinea pigs, when restimulated in vitro with PPD, showed significantly higher levels of IFN-γ mRNA, while IL-17A mRNA expression was somewhat elevated, although not significantly so, in lymph node and lung digest cells after BCG stimulation. It is known that during pulmonary BCG infection of mice, IL-17 was expressed both during the innate and adaptive phases of the immune response and the main source of IL-17 was found to be $\gamma\delta^+$ T cells [40]. Others have reported that Th17 cells were induced in BCG-immunized healthy adults vaccinated with one of the new TB candidate vaccines, MVA85A [41]. It has been reported that multidrug resistant strains (MDR) of *M. tb* induced higher levels of IL-17 T cell responses in patients with MDR TB compared to drug-susceptible strains [42].

Additional future studies will be aimed at the generation of polyclonal antibodies against rgp IL-17 by immunizing rabbits as we have reported for other guinea pig cytokines in the past [11, 13]. In vivo neutralization experiments using anti-IL-17A will be performed similar to those reported for anti-TNF-α and anti-IL-10 by our group [32, 43]. By cloning other important guinea pig cytokine genes related to the function of Th17 cells (e.g., IL-6, IL-22, IL-23), the role of those cells in the establishment of protective pulmonary $CD4^+$ T cell responses after vaccination and challenge with *M. tb* can be evaluated as has been done in mice [44]. Studies of in situ IL-17 mRNA expression in

pulmonary granulomas from *M. tb*-infected guinea pigs using laser capture microdissection will reveal the contributions of IL-17 to the development and architecture of the lesions as we have documented for other cytokines previously [45, 46]. In addition, it will be important in future studies to document the constitutive expression of IL-17 in other cell types and tissues in both BCG-vaccinated and naive guinea pigs.

In conclusion, we have deduced the complete nucleotide sequence of the guinea pig IL-17A gene and described an efficient strategy for generating recombinant guinea pig IL-17A protein that can serve as an invaluable tool for the study of the role of Th17 cells in a highly relevant animal model of TB and other pulmonary diseases.

Acknowledgments This work was supported by a subcontract from Colorado State University under NIH contract HHSN 266200400091c. The authors thank Dr. Larry Dangott of the Protein Chemistry Lab at Texas A&M University for mass spectrometry analysis.

References

1. W.H.O report. (2011). World Health Organization: Global tuberculosis control. Geneva: WHO.
2. Anderson, P., & Doherty, T. M. (2005). The success and failure of BCG—implications for a novel tuberculosis vaccine. *Nature Reviews Microbiology, 3*, 656–662.
3. Ottenhoff, T. H. M., & Kuaufmann, S. H. E. (2012). Vaccines against tuberculosis: Where are we and where do we need to go?. *PLoS Pathogens, 8*, e1002607.
4. McMurray, D. N. (2001). Disease model: Pulmonary tuberculosis. *Trends in Molecular Medicine, 7*, 135–137.
5. Turner, O. C., Basaraba, R. J., & Orme, I. M. (2003). Immunopathogensis of pulmonary granulomas in the guinea pig after infection with *Mycobacterium tuberculosis*. *Infection and Immunity, 71*, 864–871.
6. Ordway, D., Palanisamy, G., Henao-Tamayo, M., Smith, E. E., Shanley, C., Orme, I. M., et al. (2007). The cellular immune response to *Mycobacterium tuberculosis* infection in the guinea pig. *Journal of Immunology, 179*, 2532–2541.
7. Padilla-Carlin, D. J., McMurray, D. N., & Hickey, A. J. (2008). The guinea pig as a model of infectious diseases. *Comparative Medicine, 58*, 324–340.
8. Lyons, M. J., Yoshimura, T., & McMurray, D. N. (2002). *Mycobacterium bovis* BCG vaccination augments interleukin-8 mRNA expression and protein production in guinea pig alveolar macrophages infected with *Mycobacterium tuberculosis*. *Infection and Immunity, 70*, 5471–5478.
9. Skwor, T. A., Cho, H., Cassidy, C., Yoshimura, T., & McMurray, D. N. (2004). Recombinant guinea pig CCL5 (RANTES) differentially modulates cytokine production in alveolar and peritoneal macrophages. *Journal of Leukocytic Biology, 76*, 1229–1239.
10. Lasco, T. M., Cassone, L., Kamohara, H., Yoshimura, T., & McMurray, D. N. (2005). Evaluating the role of tumor necrosis factor-alpha in experimental pulmonary tuberculosis in the guinea pig. *Tuberculosis (Edinb), 85*, 245–258.
11. Jeevan, A., McFarland, C. T., Yoshimura, T., Skwor, T., Cho, H., Lasco, T., et al. (2006). Production and characterization of guinea pig recombinant gamma interferon and its effect on macrophage activation. *Infection and Immunity, 74*, 213–224.
12. Jeevan, A., Yoshimura, T., Ly, L. H., Dirisala, V. R., & McMurray, D. N. (2011). Cloning of guinea pig IL-4: Reduced IL-4 mRNA after vaccination or *Mycobacterium tuberculosis* infection. *Tuberculosis (Edinb), 91*, 47–56.
13. Dirisala, V. R., Jeevan, A., Bix, G., Yoshimura, T., & McMurray, D. N. (2012). Molecular cloning and expression of the IL-10 gene from guinea pigs. *Gene, 498*, 120–127.
14. Dirisala, V. R., Jeevan, A., Ly, L. H., & McMurray, D. N. (2013). Prokaryotic expression and in vitro functional analysis of IL-1β and MCP-1 from guinea pig. *Molecular Biotechnology, 54*, 312–319.
15. Zuniga, J., Torres-Garcia, D., Santos-Mendoza, T., Rodriguez-Reyna, T.S., Granados, J., & Yunis, E. J. (2012). Cellular and humoral mechanisms involved in the control of tuberculosis. *Clinical and Developmental Immunology,* Article ID 193923. doi: 10.1155/2012/193923.
16. Qiao, D., Yang, B. Y., Li, L., Ma, J. J., Zhang, X. L., Lao, S. H., et al. (2011). ESAT-6- and CFP-10-specific Th1, Th22 and Th17 cells in tuberculous pleurisy may contribute to the local immune response against *Mycobacterium tuberculosis* infection. *Scandinavian Journal of Immunology, 73*, 330–337.
17. Yoshida, Y. O., Umemura, M., Yahagi, A., O'Brien, R. L., Ikuta, K., Kishihara, K., et al. (2010). Essential role of IL-17A in the formation of a mycobacterial infection-induced granuloma in the lung. *Journal of Immunology, 184*, 4414–4422.
18. Torrado, E., & Cooper, A. M. (2010). IL-17 and Th17 cells in tuberculosis. *Cytokine Growth Factor Reviews, 21*, 455–462.
19. Sutherland, J. S., Jong, B. C. D., Jeffries, D. J., Adetifa, I. M., & Ota, M. O. C. (2010). Production of TNF-α, IL-12(P40) and IL-17 can discriminate between active TB disease and latent infection in a West African cohort. *PLoS One, 5*, e12365.
20. Korn, T., Bettelli, E., Oukka, M., & Kuchroo, V. K. (2009). IL-17 and Th-17 cells. *Annual Reviews of Immunology, 27*, 485–517.
21. Lin, Y., Slight, S. R., & Khader, S. A. (2010). Th-17 cytokines and vaccine induced immunity. *Seminars in Immunopathology, 32*, 79–90.
22. Iwakura, Y., Ishigame, H., Saijo, S., & Nakae, S. (2011). Functional specialization of interleukin-17 family members. *Immunity, 25*, 149–162.
23. Jeevan, A., Yoshimura, T., Foster, G., & McMurray, D. N. (2002). Effect of *Mycobacterium bovis* BCG vaccination on interleukin-1 beta and RANTES mRNA expression in guinea pig cells exposed to attenuated and virulent mycobacteria. *Infection and Immunity, 70*, 1245–1253.
24. Hansen, M. B., Nielsen, S. E., & Berg, K. (1989). Re-examination and further development of a precise and rapid dye method for measuring cell growth/cell kill. *Journal of Immunological Methods, 119*, 203–210.
25. Rio, D. C., Ares, M., Jr., Hannon, G. J., & Nilsen, T. W. (2010). *Determining the yield and quality of purified RNA (Cold Spring Harbor Protocol)*. Cold Spring Harbor, NY: Cold Spring Harbor Laboratory Press.
26. Tamura, K., Peterson, D., Peterson, N., Stecher, G., Nei, M., & Kumar, S. (2011). MEGA5: Molecular evolutionary genetics analysis using maximum likelihood, evolutionary distance, and maximum parsimony methods. *Molecular Biology and Evolution, 28*, 2731–2739.
27. Shevchenko, A., Tomas, H., Hayil, J., Olsen, J. V., & Mann, M. (2007). In-gel digestion for mass spectrometric characterization of proteins and proteomes. *Nature Protocols, 1*, 2856–2860.
28. Laskowski, R. A., MacArthur, M. W., Moss, D. S., & Thornton, J. M. (1993). PROCHECK: A program to check the stereochemical quality of protein structures. *Journal of Applied Crystallography, 26*, 283–291.

29. Ramachandran, G. N., Ramakrishnan, C., & Sasisekharan, V. (1963). Stereochemistry of polypeptide chain configurations. *Journal of Molecular Biology, 7*, 95–99.
30. Gerhardt, S., Abbott, W. M., Hargreaves, D., Pauptit, R. A., Needham, M. R., Langham, C., et al. (2009). Structure of IL-17A in complex with a potent, fully human neutralizing antibody. *Journal of Molecular Biology, 394*, 905–921.
31. García-Fruitós, E., Vázquez, E., Díez-Gil, C., Corchero, J. L., Seras-Franzoso, J., Ratera, I., et al. (2012). Bacterial inclusion bodies: Making gold from waste. *Trends in Biotechnology, 30*, 65–70.
32. Jeevan, A., Formichella, C. R., Russell, K. E., & Dirisala, V. R. (2013). Guinea pig skin, a model for epidermal cellular and molecular changes induced by UVR in vivo and in vitro: Effects on *Mycobacterium bovis* Bacillus Calmette–Guèrin vaccination. *Photochemistry and Photobiology, 89*, 189–198.
33. Kotobuki, Y., Tanemura, A., Yang, L., Itoi, S., Wataya-Kaneda, M., Murota, H., et al. (2012). Dysregulation of melanocyte function by Th17-related cytokines: Significance of Th17 cell infiltration in autoimmune vitiligo vulgaris. *Pigment Cell Melanoma Research, 25*, 219–230.
34. Jovanovic, D. V., Di Battista, J. A., Martel, P. J., Jolicoeur, F. C., He, Y., Zhang, M., et al. (1998). IL-17 stimulates the production and expression of proinflammatory cytokines, IL-beta and TNF-alpha, by human macrophages. *Journal of Immunology, 160*, 3513–3521.
35. Laan, M., Cui, Z. H., Hoshino, H., Lötvall, J., Sjöstrand, M., Gruenert, D. C., et al. (2009). Neutrophil recruitment by human IL-17 via C-X-C chemokine release in the airways. *Journal of Immunology, 162*, 2347–2352.
36. Laan, M., Prause, O., Miyamoto, M., Sjostrand, M., Hytonen, A. M., Kaneko, T., et al. (2003). Role of GM-CSF in the accumulation of neutrophils in the airways caused by IL-17 and TNF-alpha. *European Respiratory Journal, 21*, 387–393.
37. Witowski, J., Pawlaczyk, K., Breborowicz, A., Scheuren, A., Kuzlan-Pawlaczyk, M., Wisniewska, J., et al. (2000). IL-17 stimulates intraperitoneal neutrophil infiltration through the release of GRO alpha chemokine from mesothelial cells. *Journal of Immunology, 165*, 5814–5821.
38. Jeevan, A., Majorov, K., Sawant, K., Cho, H., & McMurray, D. N. (2007). Lung macrophages from bacille Calmette–Guèrin-vaccinated guinea pigs suppress T cell proliferation but restrict intracellular growth of *M. tuberculosis* after recombinant guinea pig interferon-gamma activation. *Clinical and Experimental Immunology, 149*, 387–398.
39. Jeevan, A., Bonilla, D. L., & McMurray, D. N. (2009). Expression of interferon-gamma and tumour necrosis factor-alpha messenger RNA does not correlate with protection in guinea pigs challenged with virulent *Mycobacterium tuberculosis* by the respiratory route. *Immunology, 128*, e296–e305.
40. Martin, B., Hirota, K., Cua, D. J., Stockinger, B., & Veldhoen, M. (2009). Interleukin-17-producing gammadelta T cells selectively expand in response to pathogen products and environmental signals. *Immunity, 31*, 321–330.
41. de Cassan, S. C., Pathan, A. A., Sander, C. R., Minassian, A., Rowland, R., Hill, A. V. S., et al. (2010). Investigating the induction of vaccine-induced Th17 and regulatory T cells in healthy, *Mycobacterium bovis* BCG-immunized adults vaccinated with a new tuberculosis vaccine, MVA85A. *Clinical and Vaccine Immunology, 17*, 1066–1073.
42. Basile, J. I., Geffner, L. J., Romero, M. M., Balboa, L., Sabio, Y., García, C., et al. (2011). Outbreaks of mycobacterium tuberculosis MDR strains induce high IL-17 T-cell response in patients with MDR tuberculosis that is closely associated with high antigen load. *Journal of Infectious Diseases, 204*, 1054–1064.
43. Ly, L. H., Jeevan, A., & McMurray, D. N. (2009). Neutralization of TNFα alters inflammation in guinea pig tuberculous pleuritis. *Microbes and Infection, 11*, 680–688.
44. Khader, S., Bell, G. K., Pearl, J. E., Fountain, J. J., Rangel-Moreno, J., Cilley, G. E., et al. (2007). IL-23 and IL-17 in the establishment of protective pulmonary CD4+ T cell responses after vaccination and during *Mycobacterium tuberculosis* challenge. *Nature Immunology, 8*, 369–377.
45. Ly, L. H., Russell, M. I., & McMurray, D. N. (2007). Microdissection of the cytokine milieu of pulmonary granulomas from tuberculous guinea pigs. *Cellular Microbiology, 9*, 1127–1136.
46. Ly, L. H., Russell, M. I., & McMurray, D. N. (2008). Cytokine profiles in primary and secondary pulmonary granulomas of guinea pigs with tuberculosis. *American Journal of Respiratory and Cellular Molecular Biology, 38*, 455–462.